Available online at www.sciencedirect.com
SCIENCE DIRECT®
Pergamon
Cement and Concrete Research 34 (2004) 1441–1450
CEMENT AND CONCRETE RESEARCH

Fracture of model concrete 1. Types of fracture and crack path

C. Rosselló, M. Elices*

Departamento de Ciencia de Materiales, Universidad Politécnica de Madrid, E.T.S.I. Caminos, Profesor Aranguren s/n 28040 Madrid, Spain

Received 17 March 2003; accepted 22 January 2004

Abstract

The paper presents experimental data that would serve to verify theoretical models of concrete fracture, particularly the effect of aggregate strength and mortar–aggregate interface on concrete strength, fracture paths, and deformation properties. Six types of concrete were designed and tested. All the concretes were made with the same matrix. We used two types of aggregates (spheres of the same diameter but of different strength) and three kinds of aggregate–matrix interfaces (debonded aggregates, strongly bonded, and intermediate bonded). Fracture behaviour was investigated by testing notched beams. All in all, 87 tests were performed. Detailed load–displacement and load–CMOD curves for the six types of concrete and two beam sizes are given. The different types of fracture—*intergranular*, through the matrix or the interface, or *transgranular*—are specified for the different aggregate–matrix interfaces. The properties of the matrix, aggregate, and interfaces needed to reproduce these tests numerically are provided in this paper, permitting others to check numerical models of concrete fracture.

Keywords: Concrete; Fracture; Aggregate–matrix interface; Debonding; Modelling

1. Purpose and objectives

Concrete is the most commonly used material of construction throughout the world and there is a growing need to understand its mechanical behaviour from the properties of its components, particularly the cracking and fracture behaviour [1–5]. This paper offers experimental results of this research, with the aim that they may be useful for concrete design and serve as an experimental benchmark for checking numerical models. See, for example, Ref.[6], chap. 3, Refs. [7,8], and Ref. [9], chap. 5.

The approach is at the meso-level, where the particle structure, the matrix, and the particle–matrix interface are the relevant ingredients for modelling the mechanical behaviour. This is true, particularly for the particle–matrix interface, because it is hoped that a better understanding of the concrete fracture can be grasped from more information about the interaction between the matrix and aggregates [10].

A very simple concrete—a *model concrete*—was designed: the same matrix, with cement and sand, was used in all the concretes. Two types of aggregates, hard and soft balls, of the same radius were chosen, and three types of matrix interfaces were selected looking for strong, middle, and weak adhesion. These six types of concrete have provided interesting results for understanding fracture processes.

The aim of this first paper is to provide a detailed description of the manufacture of the different types of simple model concretes, the experimental setup, testing procedures, and experimental results. Types of fracture and crack paths are also discussed. Modulus of rupture, fracture energy, and softening behaviour are dealt with in subsequent papers. It is hoped that experimental results from this first paper —particularly *load–displacement* and *load–CMOD* curves—may be helpful in checking numerical models of concrete failure.

2. The model concrete

This type of concrete is not intended to be a model—a perfect—material; the aim is to make a very simple material accessible to be modelled. With this purpose in mind, a simple aggregate was chosen—a sphere—and only a few

* Corresponding author. Tel.: +36-915433947; fax: +36-915437845.
E-mail address: melices@mater.upm.es (M. Elices).

0008-8846/$ – see front matter © 2004 Elsevier Ltd. All rights reserved.
doi:10.1016/j.cemconres.2004.01.028

Table 1
Average composition of the mortar matrix

Component	Cement	Sand	Silica fume	Plasticizer	Water
kg/m^3	655	1274	59	44	214

Table 2
Average chemical composition of the aggregate

Component	$SiO_2Al_2O_3$	K_2O	Fe_2O_3	TiO_2	CaO	MgO	Na_2O
Percentage	95	1.5	1.4	0.6	0.5	0.5	0.5

Table 3
Average composition of the model concrete

Component	Cement	Sand	Aggregate	Water	Silica fume	Plasticizer
kg/m^3	482	938	544	157	42	32
dm^3/m^3	153	354	258	157	22	26

parameters are used. Six types of concrete were prepared, with two types of aggregates and three kinds of aggregate–matrix interfaces. The matrix was always the same.

2.1. Materials

The matrix was a mortar of cement and sand, designed for a flexural strength of about 3 MPa and workable enough to manufacture the concrete samples. The cement used was of Type III Portland cement (according to ASTM and European standards). The sand was siliceous, of a size between 0.2 and 0.4 mm. Silica fume was added to increase the strength of the mortar, and a superplasticizer (Sikament 300) was added to improve its workability. The average composition of the mortar is shown in Table 1.

The aggregates were commercial spheres of mullite, used in catalysis, with an average diameter of 7.4 mm. Two types of spheres were considered for this research: the *hard* spheres, with average tensile strength of 16 MPa, were obtained after heat treatment at 1100 °C, and the *soft* spheres, with average tensile strength of 2 MPa, by a heat treatment of 100 °C for 24 h plus 650 °C for 5 h. The average chemical composition of the aggregates is shown in Table 2.

Table 4
Notched beams tests

Type of aggregate	Beam depth (mm)	Number of tests		
		Strong interface	Medium interface	Weak interface
Soft spheres	40	7	16	16
Soft spheres	75	6	6	6
Hard spheres	40	10	10	10

The matrix–aggregate interface was modified by doubling the spheres with a release agent or an epoxy resin. This surface provided two kinds of matrix–aggregate interfaces when applied to soft aggregates: *weak* interfaces (with a release agent) and *strong* interfaces (with an epoxy polymer). When applied to strong aggregates—with a hard and polished surface—the epoxy was rejected and the aggregates were debonded from the matrix, the interface being much weaker than that achieved with the release agent. The release agent used in this research was an aqueous emulsion of paraffin.

The concrete mix is shown in Table 3. The water/cement ratio, by weight, was 0.32. The percentage in volume of round aggregates was 25.8.

2.2. Sample manufacture

Beam samples were manufactured for this research. The geometry of the samples is shown in Fig. 1.

Special care was taken with the control of the aggregate–matrix interface: when using epoxy resin, its two components were blended separately and poured into a container with the aggregates, stirred until the aggregates were completely covered by the epoxy resin, and left to settle for 2 h. The release agent was mixed with the aggregates 30 min

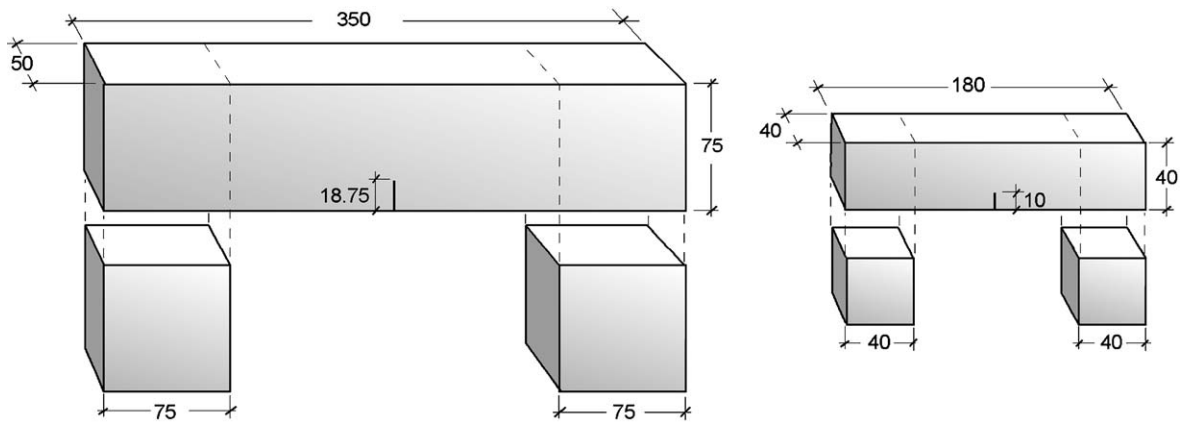

Fig. 1. Beam geometry: two types of beams (depth, $D = 40$ mm and $D = 75$ mm) were tested. Notch depth was always $D/4$. Small cubes ($40 \times 40 \times 40$) and prisms ($75 \times 75 \times 50$) from broken beams were used for indirect tensile tests.

before the manufacture of the concrete. When no treatment was applied, the aggregates were immersed in water for 2 h up to saturation.

The water content was critical. As the selected mix had a low water/cement ratio (0.3) and ambient humidity was not controlled, it was found that a small decrease in water content prevented the correct casting of the specimens. In order to avoid water evaporation, it was decided to cool the water before the manufacturing process so that during the mix its temperature remained below 5 °C. With this procedure, a mix with a proper texture for casting and vibration was obtained. Good repetition was achieved.

Thorough mixing was essential to ensure consistent workability, homogeneity, and strength. Components were added to the mixer in the following order: first, previously homogenized cement and silica fume were measured into the mixer container. Water with superplasticizing additive was added and the mixture was stirred at low velocity for 1 min. Then, the sand was added and mixed for 1 min, and finally, the mix was subjected to fast rotation for 1 min.

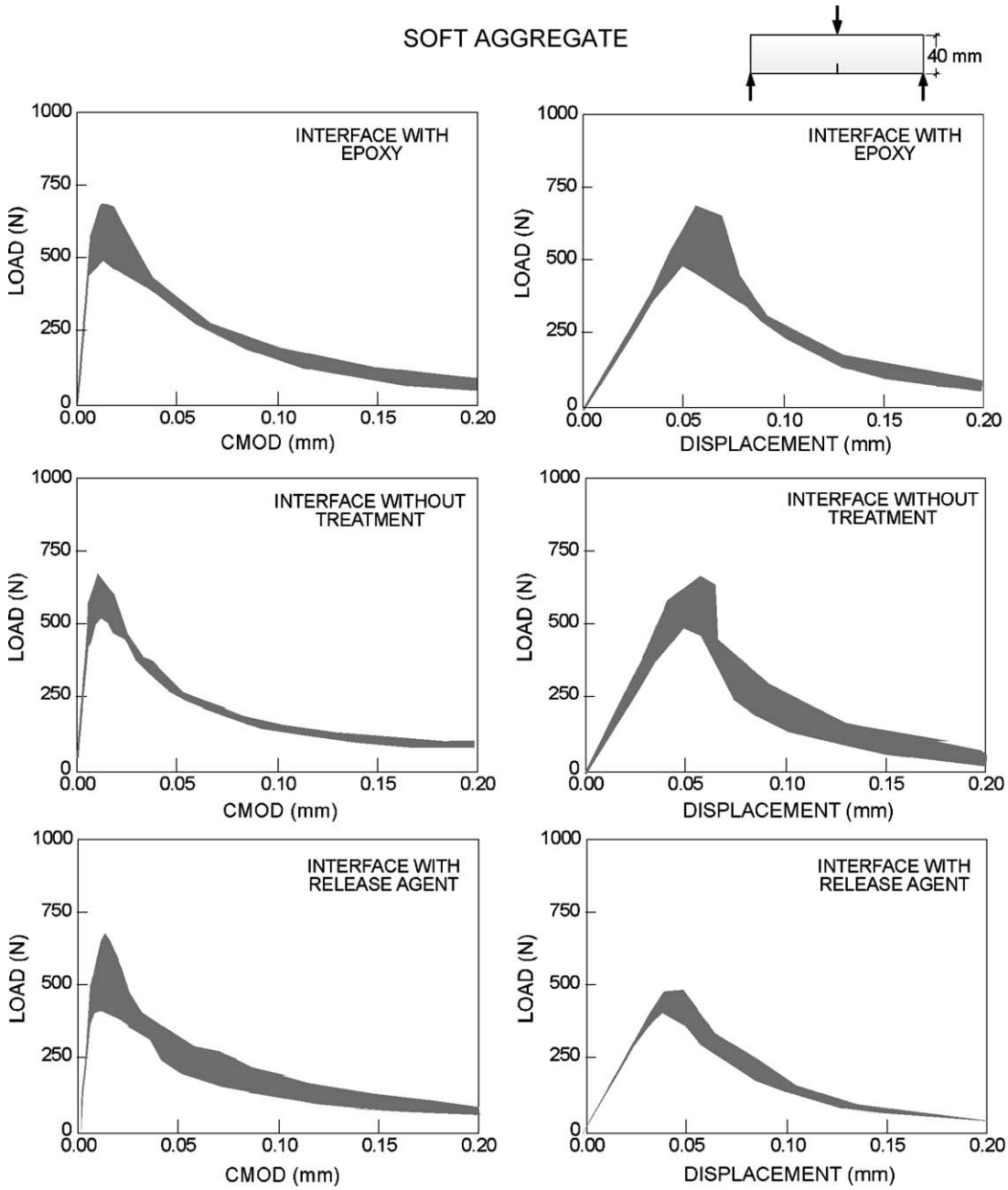

Fig. 2. Load–CMOD and load–displacement curves for small notched beams ($D = 40$ mm) of concrete with soft aggregates and three different aggregate–matrix interfaces.

The mixer was stopped and the aggregates were brought in and stirred by hand to avoid any damage.

Metallic casting forms were greased with a release agent and fixed to a vibration table before the start of the casting. The casting of the specimens was done in two layers in both types of sample. The beams were always filled sideways to avoid gradients of composition along their width. The vibration time was 10–15 s per layer, trying to avoid segregation. The maximum time between the end of the mix and the filling of the last specimen was always less than 20 min.

Curing was done in the following way: watertight sheeting was placed over the specimens. They remained in this water-saturated atmosphere for 24 h to avoid shrinkage and cracking. The specimens were then taken out of the forms, marked, and immersed in the laboratory water pools until notching.

The notches were milled with a diamond steel disc of 175-mm diameter and 1.5-mm width at a rotation velocity of 100 rpm. The advance velocity was 850 mm/min; water-soluble oil was used as coolant. The notch depth, as shown in Fig. 1, was always 0.25 of the beam depth.

Cubes and prisms for indirect tensile tests were manufactured from the broken parts of the bending tests, as shown in Fig. 1.

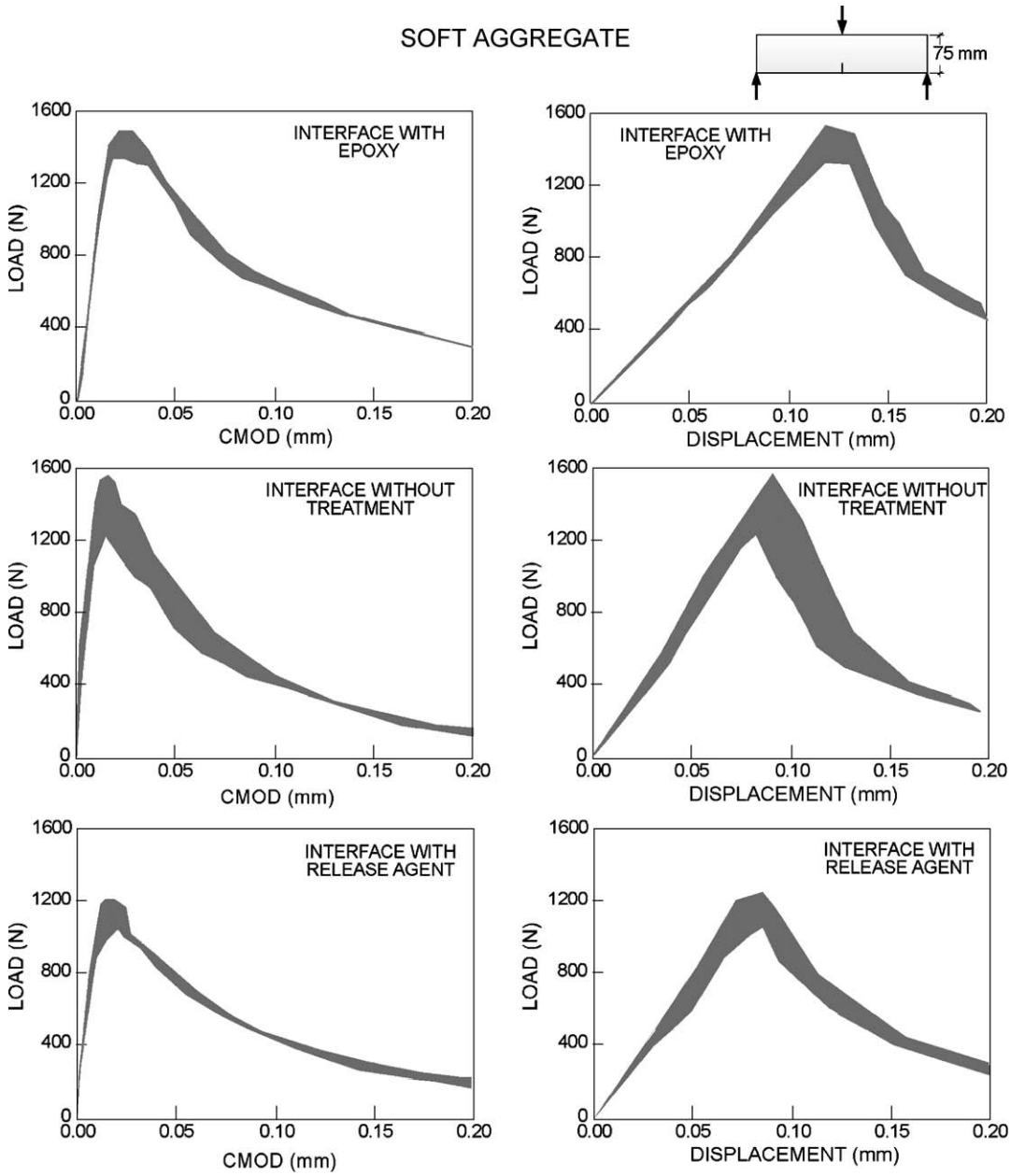

Fig. 3. Load–CMOD and load–displacement curves for large notched beams ($D = 75$ mm) of concrete with soft aggregates and three different aggregate–matrix interfaces.

3. Experimental work

The fracture behaviour of the model concrete was studied by testing notched beams loaded at three points, as recommended by RILEM [11]. Possible sources of experimental errors in this test, as detailed by Planas, Elices, and Guinea [12–14], were taken into account.

Stable three-point bend tests were performed in a 1 MN servohydraulic testing machine INSTRON 1275, run in crack mouth opening displacement (CMOD) control mode. Load was measured with a 5-kN load cell of 5 N resolution and 0.25% accuracy. An extensometer, with ±2.5-mm travel and ±0.2% error at full-scale displacement, was used to measure the CMOD. Two transducers, with ±2.0-mm travel and ±0.2% error at full-scale displacement, were used to measure the load-point displacement of the applied force.

Beams of the model concrete made from soft spheres were tested in two sizes: of 40- and of 75-mm depth. Concrete from hard spheres was tested only with notched beams of the small size, i.e., 40-mm depth. The geometry of these beams appears in Fig. 1. The number of beams tested, according to the nature of the aggregate–matrix interface, is shown in Table 4. All in all, 87 beams were tested.

The main results are recorded in Figs. 2, 3, and 4. Fig. 2 shows the results of load–CMOD and load–displacement

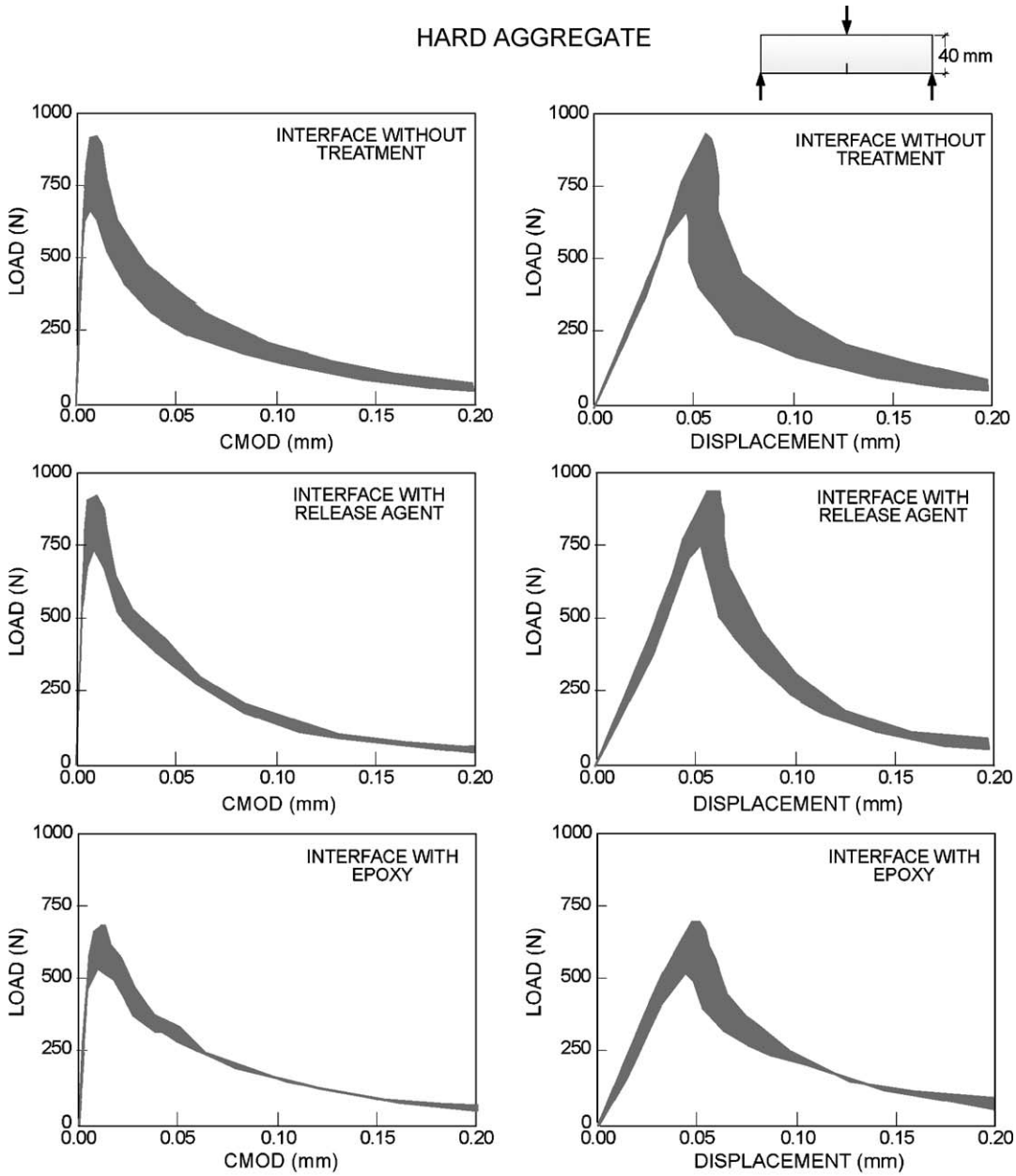

Fig. 4. Load–CMOD and load–displacement curves for small notched beams (D = 40 mm) of concrete with hard aggregates and three different aggregate–matrix interfaces.

Table 5
Mechanical properties of matrix and aggregates

	Matrix	Hard aggregate	Soft aggregate
Young modulus (GPa)	31 ± 2	19 ± 2	2.1 ± 0.5
Tensile strength (MPa)	4.7 ± 2	16 ± 2	1.7 ± 0.3
Fracture energy (J/m^2)	52 ± 6	(not measured)	(not measured)

in small notched beams ($D = 40$ mm) made from soft aggregates and with three different aggregate–matrix interfaces. Fig. 3 depicts the results of the same tests performed with larger notched beams ($D = 75$ mm). Similar results, load–CMOD and load–displacement curves, of the concrete with hard aggregates are shown in Fig. 4.

All the 87 experimental results lie within the grey bands shown in the figures. The experimental scatter is seen to be acceptable for this kind of quasi-brittle cementitious material.

Table 5 shows the basic parameters measured in the matrix and aggregates that can be useful when modelling the concrete at the meso-level.

Bonding between matrix and aggregates, with different coatings, was measured by tensile tests of small samples with spheres placed in a plane normal to the tensile force (as shown in Fig. 5) following a procedure suggested by van Mier et al. [15] for beams. The spheres were glued (the lower half) to an epoxy-based polymer and the upper half was bonded to the mortar after the pertinent coating. Only tests in which fracture took place by debonding were analyzed, and the debonded surface was measured to compute the specific debonding energy.

The debonding test provided a rough estimation of the specific strength of the aggregate–matrix interfaces. The results are summarized in Table 6.

4. Discussion of the fracture paths

When testing notched beams, fracture is generated at the notch root where the stress concentration is maximum. The crack path follows the energetically most favourable option: cracking the aggregates, when they are softer than the matrix, or surrounding them, when they are stronger than the matrix. The interface between matrix and aggregate also affects the tortuousity of the crack path. All these aspects are considered in the next sections.

4.1. Type of fracture

Concrete made with soft aggregates displays two types of fracture surfaces: *transgranular* fracture, when the crack path cuts the aggregates, and *intergranular* fracture, when the crack skirts them. In general, a mixture of both types appears. The percentage of each type is strongly dependent on the nature of the interface between matrix and aggregate.

An index that gives an idea of the type of fracture is the percentage of aggregates on the broken section (PA), defined as:

$$\mathrm{PA} = \frac{\text{projected surface of aggregates}}{\text{projected broken surface}}$$

When the PA is lower than the average value of a concrete with homogeneously distributed aggregates (25.8% in our model concrete), this means that the crack has bypassed the aggregates and found its way mainly through the matrix, an indication of intergranular fracture. On the contrary, PA above 25.8% is indicative of transgranular fracture or extensive debonding. The meaning of the PA index is depicted as an inset in Fig. 6b.

Fig. 6a shows the percentage of broken beams made with soft aggregates as a function of PA. The average is above 25.8%, and reflects a predominance of transgranular and/or debonding fracture.

Fig. 6b is of concrete with hard aggregates stronger than the matrix. The average PA, well below 25.8%, shows that the crack runs mainly through the matrix and that fracture is intergranular. The small percentage of beams with PA above 25.8% is due to debonding of the aggregates and reflects a very weak matrix–aggregate interface.

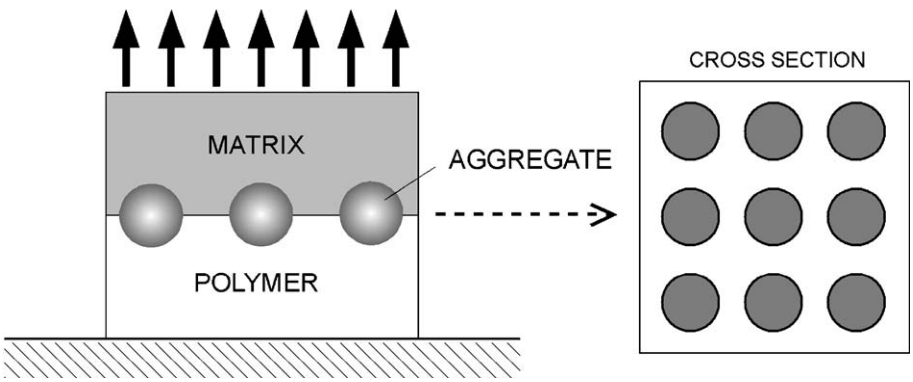

Fig. 5. Sketch of the test for measuring the bonding between aggregate and matrix.

Table 6
Estimated debonding energies (J/m^2) of interfaces

Type of aggregate	Surface treatment		
	Epoxy	None	Release agent
Soft	>26	26 ± 10	0
Hard	0	30 ± 10	30 ± 10

4.2. Influence of the matrix–aggregate interface

Three kinds of matrix–aggregate interfaces are considered in concretes with soft and hard aggregates. The purpose was to achieve weak interfaces (where the aggregates are poorly bonded to the matrix), strong interfaces (where adhesion between matrix and aggregate is very good), and intermediate ones.

Another index, related to the matrix–aggregate interface that helps in classifying fracture modes, is the percentage of broken aggregates (PBA) in the broken section, defined as:

$$\mathrm{PBA} = \frac{\text{projected surface of broken aggregates}}{\text{projected surface of aggregates}}$$

When the PBA is above 50%, the dominant type of fracture is transgranular, and intergranular if PBA is below 50%. The meaning of the PBA index is depicted as an inset in Fig. 7a.

In concretes made from soft spheres, Fig. 7a shows PBA as a function of the type of matrix–aggregate interface. In strongly bonded aggregates, the crack runs through the aggregates and all the spheres in the fracture section appear broken (PBA = 100%). When aggregates are weakly bonded—this is achieved with a release agent—the crack runs mainly through the interface and the PBA is low (PBA ≈ 5%). Intermediate PBA (≈ 50%) is recorded for aggregates with no surface treatment.

In concretes made with hard spheres, no aggregate failure was detected and all fractures were intergranular; crack paths ran through the matrix when the interface was strong (particles were well bonded to the matrix) and partly through the matrix and along the interfaces when the interface was weak, a fact reflected in Fig. 7b. This figure shows PA as a function of matrix–aggregate interface, instead of PBA, because there were no broken aggregates.

It was mentioned in Section 2.1 that the behaviour of the interfaces differed between soft and hard spheres, although the surface treatment was similar: soft spheres with an epoxy treatment provided strong interfaces, and hard spheres with the same treatment yielded poor interfaces. In hard spheres, the adherence of the epoxy was almost nil and most of the particles were debonded, as shown in Fig. 8a. Soft spheres, on the contrary, achieved good bonding with the matrix, as shown in Fig. 8b, where no cracks are observed (notice the higher magnification and the absence of debonding). When the spheres were daubed with a release agent, the opposite effect was found; Fig. 8c shows good bonding between hard spheres and matrix, while in Fig. 8d, some cracks are observed in the interface between soft spheres and matrix. This different behaviour is due to the different properties of the surfaces of the spheres, particularly porosity and roughness, acquired during aggregate manufacture.

4.3. Influence of the type of fracture test

Indirect tensile tests (splitting tests), performed to measure the tensile strength, provided additional information

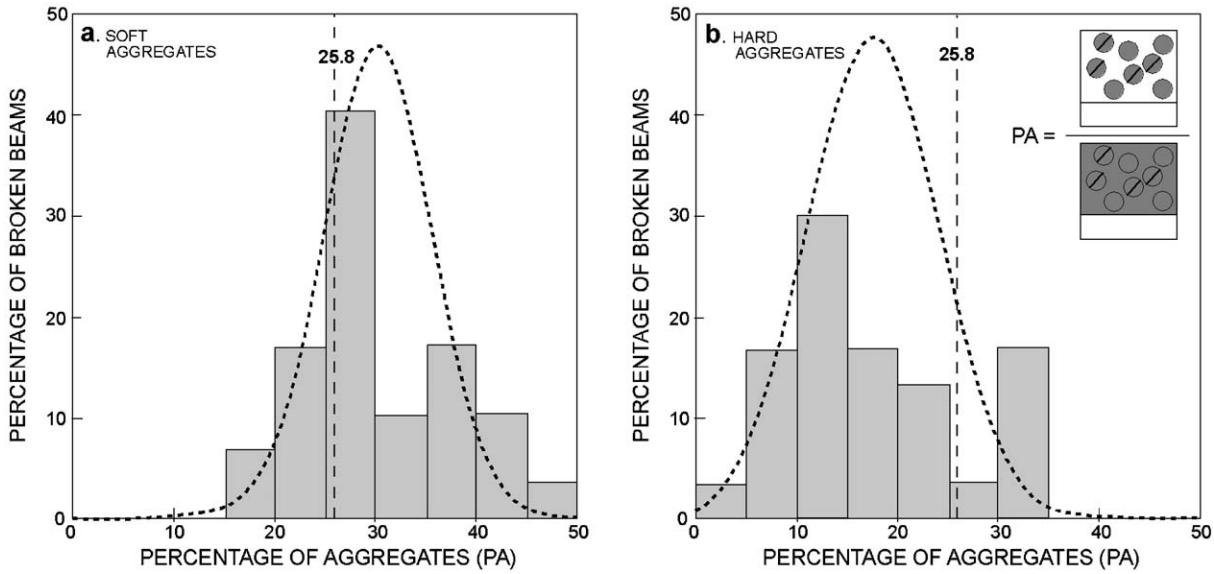

Fig. 6. (a) Percentage of broken beams (made with soft aggregates) as a function of the PA on the broken section. (b) Percentage of broken beams (made with hard aggregates) as a function of PA.

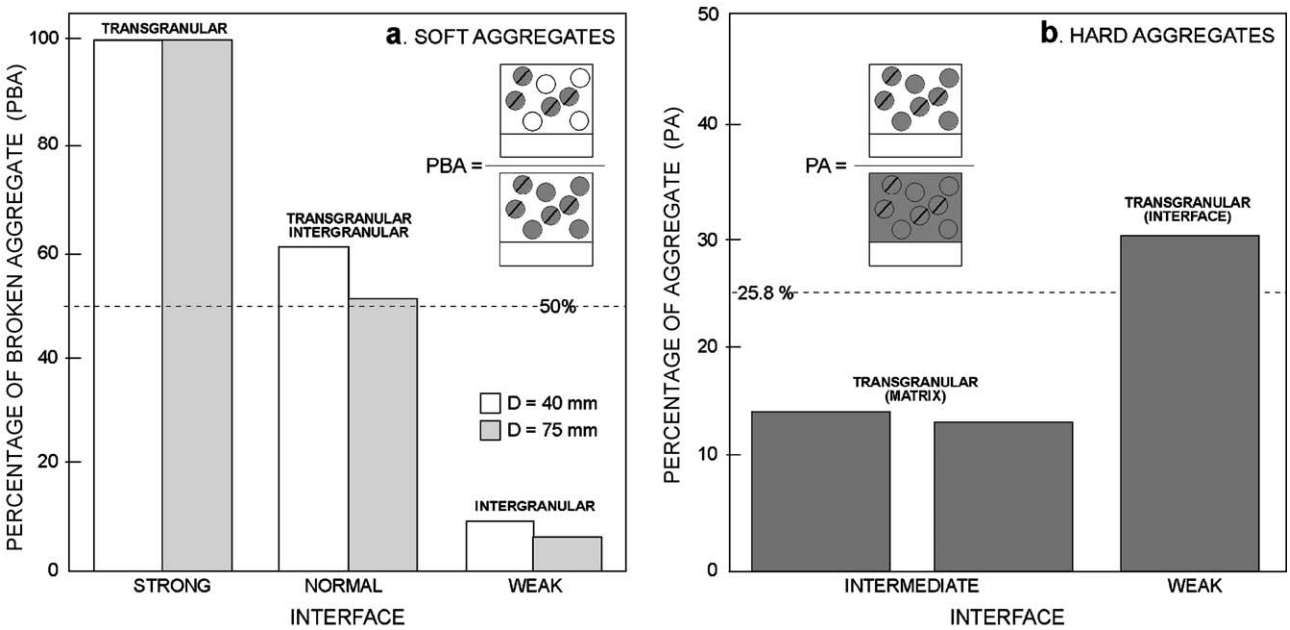

Fig. 7. (a) PBA in the broken section as a function of the matrix–aggregate interface for concrete with soft aggregates. (b) PA in the broken section as a function of the matrix–aggregate interface for concrete with hard aggregates.

about the types of fracture, particularly for concretes made with soft aggregates in which some particles break.

Comparison of fracture surfaces from bending tests and splitting tests may give some hints on the influence of the type of test on the mechanisms of fracture. The PBA was used for this purpose. Fig. 9 shows this index for both tests (bending and splitting) performed with small beams ($D = 40$ mm) and large beams ($D = 75$ mm) made with concrete with soft aggregates. Each point in the figure corresponds to one type of interface and beam size. The slope of the correlation

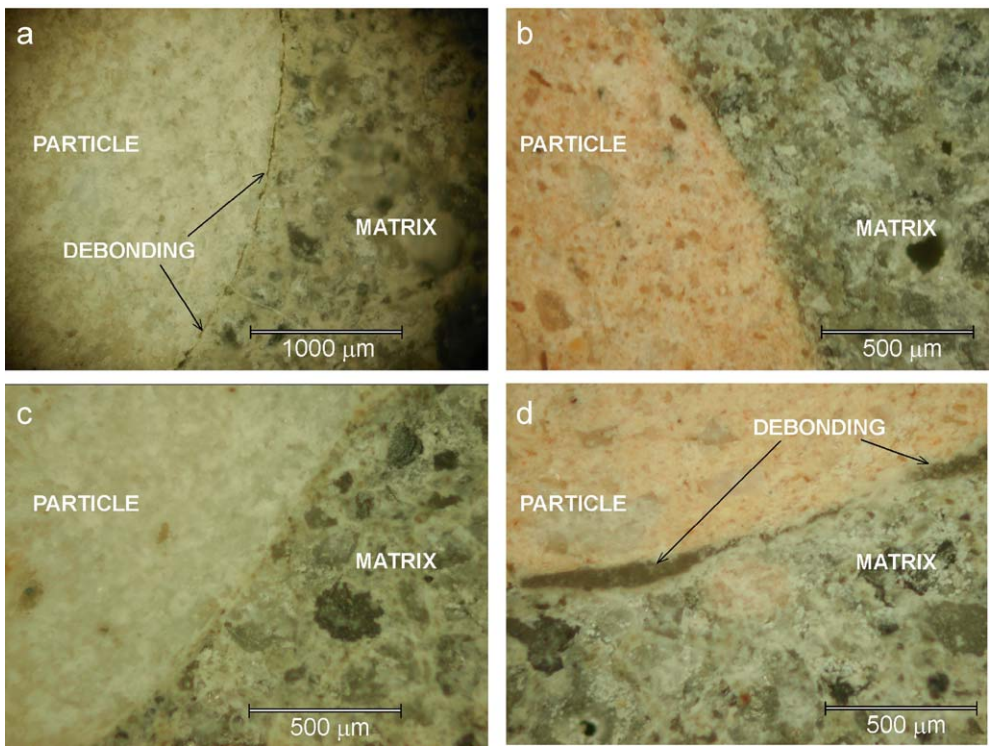

Fig. 8. Optical photographs of aggregate–matrix interfaces. (a) Hard particles with epoxy. (b) Soft particles with epoxy. (c) Hard particles with release agent. (d) Soft particles with release agent.

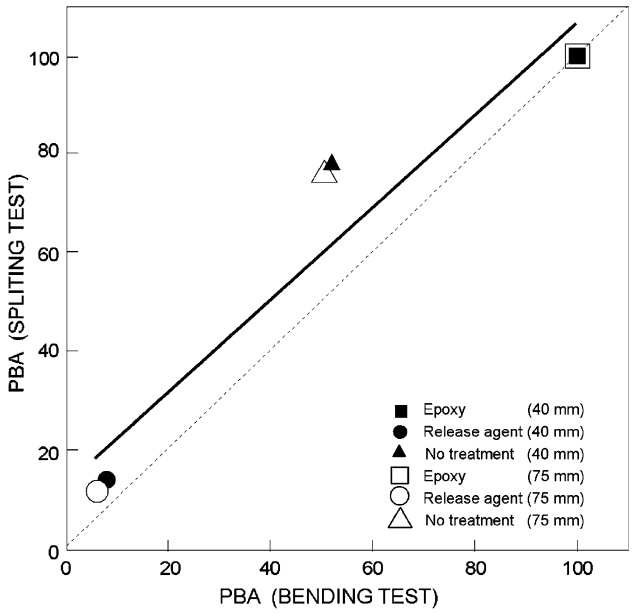

Fig. 9. PBA in bending and splitting tests.

line was 0.93 and its regression coefficient was 0.96. Both figures indicate that the type of fracture was the same, regardless of the type of test.

5. Summary and conclusions

The main contributions of this work may be summarized as follows:

- A simple model concrete was designed and tested: the matrix was always the same, two types of aggregates (spheres of the same diameter) were used, and three kinds of aggregate–matrix interfaces were considered. All in all, 87 tests were done. The main data of the matrix, aggregate, and interfaces needed to reproduce numerically these tests are provided.
- Load–CMOD and load–displacement in notched beams were measured: curves are shown in Figs. 2, 3, and 4. For soft aggregates, three kinds of interfaces and two sizes were tested. For hard aggregates, one size and three kinds of interfaces (although in practice only two were different) were also tested. These curves show scatter bands limited by the extreme values measured during the experiments. Given the nature of this material, the results are fairly repetitive. Rupture loads and critical values of CMOD and displacement, among other relevant parameters, can be inferred from these figures.
- Different types of fracture are recorded, due to the nature of the aggregate and the type of matrix–aggregate interface. These types of fracture should be obtained as an output of the numerical modelling. For concretes made with soft aggregates and strong interfaces, all the aggregates in the crack path were broken; when the interface was weak, only 10% of the aggregates broke, and 50% (on average) when the interfaces were normal. The crack path in concrete with strong aggregates was always intergranular, but some differences were observed according to the aggregate–matrix interface; with normal interfaces, the average percentage of aggregates in the cracked section was 10%, whereas with weak interfaces it was almost 30%.

As the purpose of this research was to provide experimental results that could be used to check numerical models of concrete failure, it can be concluded that the results shown in this paper are repetitive enough to serve as an experimental benchmark.

In addition, there is increasing awareness that tensile strength and elastic modulus are not sufficient to characterize the mechanical response of concrete when ductility or toughness are of concern, and that in these circumstances, concrete has to be designed with higher values of fracture energy (related to the area under load–displacement curves). From the measured curves, it appears that the highest values of toughness were obtained with strong aggregates well bonded to the matrix, and that on increasing the strength of the matrix–aggregate interface, toughness also increases.

Acknowledgements

The authors gratefully acknowledge useful discussions with Profs. Jaime Planas and Gustavo V. Guinea. Support for this research was provided by the Spanish Ministry of Ciencia y Tecnología, under grants MAT2000-1355 and FEDER UNPM 00-33-004.

References

[1] Z.P. Bazant, J. Planas, Fracture and Size Effect in Concrete and other Quasibrittle Materials, CRC Press, USA, 1998.
[2] B. Cotterell, Y.W. Mai, Fracture Mechanics of Cementitious Materials, Blackie Academic and Professional, UK, 1996.
[3] S.P. Shah, S.E. Swartz, C. Ouyang, Fracture Mechanics of Concrete, Wiley, USA, 1995.
[4] B.L. Karihaloo, Fracture Mechanics and Structural Concrete, Longman, UK, 1995.
[5] J.G.M. van Mier, Fracture Processes of Concrete, CRC Press, USA, 1997.
[6] F.H. Wittmann (Ed.), Fracture Toughness and Fracture Energy of Concrete, Elsevier, The Netherlands, chap. 3 (1986) 89–213.
[7] A. Carpinteri (Ed.), Applications of Fracture Mechanics to Reinforced Concrete, Elsevier, UK, 1992.
[8] F.H. Wittmann (Ed.), Numerical Models in Fracture Mechanics of Concrete, A.A. Balkema, The Netherlands, 1993.
[9] Z.P. Bazant, Z. Bittnar, M. Jirasek, J. Mazars (Eds.), Fracture and Damage in Quasibrittle Structures, E & FN Spon, UK, chap. 5 (1994) 343–417.
[10] G.V. Guinea, K. El-Sayed, C.G. Rocco, M. Elices, J. Planas, The effect of bond between the matrix and aggregates on the cracking

mechanism and fracture parameters of concrete, Cem. Concr. Res. 32 (2002) 1961–1970.
[11] RILEM Draft, 50 FMC draft recommendation, Determination of the fracture energy of mortar and concrete by means of three-point bend tests on notched beams, Mater. Struct. 18 (106) (1985) 285–290.
[12] G.V. Guinea, J. Planas, M. Elices, Measurement of the fracture energy using three-point bend tests: Part 1. Influence of experimental procedures, Mater. Struct. 27 (1992) 99–105.
[13] J. Planas, M. Elices, G.V. Guinea, Measurement of the fracture energy using three-point bend tests: Part 2. Influence of the bulk energy dissipation, Mater. Struct. 25 (1992) 305–312.
[14] M. Elices, G.V. Guinea, J. Planas, Measurement of the fracture energy using three-point bend tests: Part 3. Influence of cutting the P-d tail, Mater. Struct. 25 (1992) 327–334.
[15] J.P.G. van Mier, E. Schlangen, A. Vervuurt, M.R.A. van Vliet, Damage analysis of brittle disordered materials: Concrete and rock, in: A. Bakker (Ed.), Proceedings ICM-7, Delft Univ. Press, The Netherlands, 1995, 101–110.